
Monograph:
Edwards, J.B. and Zhou, B.M. (1983) Analysis of the Transfer Function Model of Tray-Type Binary Distillation Columns with Liquid Hydraulic Delay. Research Report. ACSE Report 234 . Dept of Automatic Systems Control

---

ANALYSIS OF THE TRANSFER FUNCTION MODEL OF TRAY-TYPE BINARY DISTILLATION COLUMNS WITH LIQUID HYDRAULIC DELAY

By

J.B. Edwards and B.M. Zhou

Department of Control Engineering,
University of Sheffield,
Mappin Street, Sheffield S1 3JD.

Research Report No. 234

July 1983

1. Introduction

The companion paper (1) has deduced a transfer function model describing the composition dynamics of tray-type binary distillation columns analytically. It gave consideration to the effect of hydraulic delay and predicted the dynamic behaviour of a more-or-less first order lag nature.

Although that model was very tedious, the computed results showed that the effect of the hydraulic factor was approximately equivalent to adding a pure time lag unit into the model. Moreover, the Bode diagrams of the elements of that transfer function matrix (T.F.M) showed that a better way to approximate this system was to use a first order lag unit in series with a time lag.

In engineering design a complicated or unknown model is often reduced to a first or second order lag in series with a pure time lag. So this research has provided some support for it.

In this present investigation, which is a continuation of the preceding companion paper (1), the dynamic behaviour of that transfer function model is further analysed by both frequency and time domain techniques. The inverse Nyquist loci and the numerical computing results further reveal their dynamic behaviour to be of more or less first order-lag nature and moreover, this behaviour is shown quantitatively by means of the Least Square Method (L.S.M.).

A more exact transfer function model is deduced in the present research by solving directly the difference equationswhich is the better way of describing a tray-type distillation column because of its spatially discrete nature in real life.

2. Frequency Domain Analysis

The transfer function matrix of the terminal compositions to the input of terminal liquid and vapour flow rate has the form as follows(1):

$$Q = GF$$

where

$$Q = \begin{pmatrix} y_o \\ x'_o \end{pmatrix} \text{ is the terminal composition vector}$$

$$F = \begin{pmatrix} \ell_o \\ v \end{pmatrix} \frac{c}{V_r} \text{ is the flow vector}$$

$$G = \begin{pmatrix} G_{11} & G_{12} \\ G_{21} & G_{22} \end{pmatrix} \text{ is a 2x2 transfer function matrix}$$

$$G_{11} = \frac{\{(1+p)\phi + \phi'\}\phi_1 + \phi\,\phi_3}{\phi^2 - \{(1+p)\phi + \phi'\}^2}$$

$$G_{12} = \frac{\{(1+p)\phi + \phi'\}\phi_2 + \phi\,\phi_4}{\phi^2 - \{(1+p)\phi + \phi'\}^2}$$

$$G_{21} = \frac{\{(1+p)\phi + \phi'\}\phi_3 + \phi\phi_1}{\phi^2 - \{(1+p)\phi + \phi'\}^2}$$

$$G_{22} = \frac{\{(1+p)\phi + \phi'\}\phi_4 + \phi\phi_2}{\phi^2 - \{(1+p)\phi + \phi'\}^2}$$

$$\phi = \cosh\sqrt{p}\,N + \frac{\varepsilon + Tp}{\sqrt{p}}\sinh\sqrt{p}\,N$$

$$\phi' = \sqrt{p}\sinh\sqrt{p}\,N + (\varepsilon + Tp)\cosh\sqrt{p}\,N$$

$$\phi_1 = \{(p^2T_\ell^2 - pT_\ell + 1)\alpha\, e^{-(N-1)pT_\ell} - e^{-NpT_\ell}$$
$$+ (\alpha T_\ell e^{pT_\ell} + \alpha pT_\ell e^{pT_\ell} - \alpha e^{pT_\ell} + T_\ell e^{-2NpT_\ell})\sqrt{p}\sinh\sqrt{p}N$$
$$+ (\alpha pT_\ell e^{+pT_\ell} - \alpha e^{pT_\ell} - \alpha p e^{pT_\ell} + e^{-2NpT_\ell})\cosh\sqrt{p}N\}/(p-p^2T_\ell^2)$$

$$\phi_2 = \{\sqrt{p}\sinh\sqrt{p}N + (p-\varepsilon)\cosh\sqrt{p}N + (p+2)\varepsilon/2\}/p$$

$$\phi_3 = \{(pT_\ell + p+1)e^{-NpT_\ell} - \alpha e^{-(N-1)pT_\ell} - 0.5(\alpha+1)(p-p^2T_\ell^2)e^{-NpT_\ell}$$
$$- (\alpha T_\ell e^{pT_\ell} + T_\ell e^{-2NpT_\ell} + pT_\ell e^{-2NpT_\ell} + e^{-2NpT_\ell})\sqrt{p}\sinh\sqrt{p}N$$
$$+ (\alpha e^{pT_\ell} - e^{-2NpT_\ell} - pe^{-2NpT_\ell} - pT_\ell e^{-2NpT_\ell})\cosh\sqrt{p}N\}/(p-p^2T_\ell^2)$$

$$\phi_4 = \{\alpha\sqrt{p}\ \sinh\sqrt{p}N + (\alpha p + \varepsilon)\ \cosh\sqrt{p}\ N - \varepsilon\}/p$$

It is easty to prove from above results that when hydraulic delay T equals to zero the following equalities are tenable:

$$\phi_2 = -\phi_3 \text{ and } \phi_4 = -\phi_1.$$

This leads to $G_{12} = -G_{21}$ and $G_{22} = -G_{11}$ and in this case the T.F.M. can be reformed as a diagonal form, i.e.

$$Q' = G'F'$$

where

$$Q' = \begin{pmatrix} y_o - x'_o \\ y_o + x'_o \end{pmatrix} \qquad F = \begin{pmatrix} v + \ell_o \\ v - \ell_o \end{pmatrix} \frac{c}{V_1}$$

$$G' = \begin{pmatrix} G'_{11} & G'_{12} \\ G'_{21} & G'_{22} \end{pmatrix}$$

$$G'_{11} = 0.5(G_{11} + G_{12} - G_{21} - G_{22})$$
$$G'_{12} = 0.5(G_{12} - G_{11} + G_{21} - G_{22})$$
$$G'_{21} = 0.5(G_{11} + G_{12} + G_{21} + G_{22})$$
$$G'_{22} = 0.5(G_{12} - G_{11} - G_{21} + G_{22})$$

The equalities $G_{12} = -G_{21}$ and $G_{22} = -G_{11}$ lead to $G'_{12} = G'_{21} = 0$ i.e. the T.F.M. (G') at $T_\ell = 0$ is diagonal. In the general case, however the hydraulic delay must be involved and the T.F.M. (G') ceases to be diagonal. In fact it is not even diagonally dominant. Let $G^* = (G')^{-1}$. By ploting the inverse Nyquist diagrams of the elements G^*_{11} and G^*_{22} of the main diagonal of inverse matrix G^*, then superimposing on these diagrams circles centred at each particular frequency value on these loci with radii equal to the $|G^*_{12}(\omega)|$ and $|G^*_{21}(\omega)|$ respectively, we can find (shown in Fig. 3) that the band swept out by the circles on the locus of G^*_{22} (Fig. 3.2) contains the origin. This means the system denoted by G' is

not to be diagonally dominant. Because only the liquid delay is involved, the elements G_{12} and G_{22} which take bottom vapour flow as input are independent of T_ℓ.

2.1 Inverse Nyquist Loci:

It was found from the Bode diagrams in the companion research (1) that the composition-flow system denoted by T.F.M. (G) has very low corner frequencies ($\omega_c \leq 0.007^*$). Furthermore if the vapour moler flow is set to be $V_r = 10$ and the controller gain is $K_c = 20$ (this value is very big in practice) then under the conditions $\alpha = 1.1$, $T = 1.0$, $N = 10$ and $T_\ell = 0.2$ (In this case the composition gradient will be $c = 0.023$), we can get the closed-loop cut-off frequency by computing ($\omega_{cf} \leq 0.08$). All these show the fact that this system (G) is a low-pass filter and therefore studying its low frequency behaviour has more important significance. We choose the frequency range from 0 to 0.2 which is wide enough.

From the inverse Nyquist loci (Fig. 1) of each element of G at the same condition as above it can also be seen that they are all shaped like spirals and the locus of the element G_{21} rotates more quickly than the others. Therefore, just like the prediction from the Bode diagram as before, we can conclude again from inverse Nyquist loci that the better way to approximate the complicated model is to use a first order lag unit in series with a time lag, and that these time lags except for that of G_{21} are very small in comparison with their time constants.

2.2 Least Square Analysis:

Using Least quare Method (Appendix 1) at low frequency under the conditions $\alpha = 1.1$ ($\varepsilon = 0.1$), $T = 1.0$, $N = 10$ and $T_\ell = 0.2$, we can get a set

*All frequencies used in this research are the product of the true frequency t and the stage residence time T_x whose value is from 5 to 30 sec.(4).

of first order lag models as follows:

$$G_{11} = \frac{120.e^{-0.75p}}{164p + 1}$$

$$G_{12} = \frac{121.e^{-0.66p}}{176p + 1} \qquad (1)$$

$$G_{21} = \frac{129.e^{-4.2p}}{180.p + 1}$$

$$G_{22} = \frac{113.e^{-0.63}}{148p + 1}$$

The complex correlation coefficients are very near to 1.0 ($\zeta > 0.99$) i.e. the error is very small. In fact, the inverse Nyquist loci of these approximate models are very coincident with those of true models as shown in Fig. 1.

It can be seen from above results that the long distillation column system is a slow process with large time constants and that the dead times except for that of G_{21} are very small in comparison with the time constants so that they can be neglected in practice. In fact these time lags are not really existing, they are only the pseudo time lag used to reduce a high order or other type of complicated model. Furthermore, the computing results in different stage number and different hydraulic time constant show that the dead time of the element G_{21} is in direct proportion to stage number N and hydraulic time constant T_ℓ, i.e. $pT = 2NT_\ell$. This is in accord with the physical mechanism involved in which the reflux must pass through $2 \cdot N$ stages to get to the bottom of the column.

Fig. 4 shows the inverse Nyquist loci of element G_{21} in different hydraulic time constant. T_ℓ = 0.0, 0.2, 0.4 and 0.6 respectively. It can be seen from this diagram that the phase angle difference θ_{20} between the locus of T_ℓ = 0.2 and that of T_ℓ = 0.0 is equal to the difference θ_{42} between T_ℓ = 0.4 and T_ℓ = 0.2 at the same frequency ω = 0.135 and so is the difference θ_{64} between T_ℓ = 0.6 and T_ℓ = 0.4. i.e. $\theta_{20} = \theta_{42} = \theta_{64} \doteq 20^\circ$ and their magnitudes are roughly equal to one another. This further

shows the time delay of element G_{21} to be directly proportional to hydraulic time constant T_ℓ.

2.3 Taylor Series Expansion:

According to the final value theorem, the value of each element at zero frequency (assume the input to be unit step) should be its steady state gain which is independent of hydraulic delay.

$$K_{11} = -K_{22} \doteq \frac{(3\alpha+1)\varepsilon N^2 + 4\alpha^2 N + 4 + 5\varepsilon}{4\varepsilon^2 N + 2\varepsilon(\alpha+1)} \triangleq K_1$$

$$K_{21} = -K_{12} \doteq \frac{(\alpha+3)\varepsilon N^2 + 4\alpha^2 N + 4 + 5\varepsilon}{4\varepsilon^2 N + 2\varepsilon(\alpha+1)} \triangleq K_2 \qquad (2)$$

Now that the effect of hydraulic delay is equivalent to adding a time lag into system [1] and the dead time $DT = 2NT_\ell$ as above, we can first expand each element of T.F.M as a first order lag (ignoring the hydraulic delay) at low frequency then put a time lag into element G_{21}. Expanding the reciprocal of each element of T.F.M (G) into Taylor series in the vicinity of zero frequency (setting $T_l = 0$) and truncating second and higher terms yield:

$$G_{11}^{-1} = -G_{22}^{-1} = A_1 + B_1 p = A_1(1 + p B_1/A_1)$$

$$G_{21}^{-1} = -G_{12}^{-1} = A_2 + B_2 p = A_2(1 + p B_2/A_2) \qquad (3)$$

where

$A_1 = K_1^{-1}$ and $A_2 = K_2^{-1}$ are steady state gain expressed in eq. (2).

$$B_1/A_1 = T_1$$

$$\doteq \frac{(17+62\varepsilon)\varepsilon^2 N^4 + (32+125\ )\varepsilon^2 N^3 + (26+200\varepsilon)\varepsilon N^2 + (8+120\varepsilon T)N}{(8+6\varepsilon)\varepsilon^4 N^3 + (24+54\varepsilon)\varepsilon^3 N^2 + (24+100\varepsilon)\varepsilon^2 N + (8+52\varepsilon)\varepsilon}$$

$$B_2/A_2 = T_2$$

$$\doteq \frac{(4+8\varepsilon)\varepsilon^3 N^4 + (8+30\varepsilon)\varepsilon^2 N^3 + (7+50\varepsilon)\varepsilon N^2 + (2 + 40\varepsilon T)}{2\varepsilon^4 N^3 + (6+11\varepsilon)\varepsilon^3 N^2 + (6+26\varepsilon)\varepsilon^2 N + (2 + 20\varepsilon)\varepsilon}$$

where T_1 and T_2 are time constant.

In this way all the elements of T.F.M can be expanded into first order lag whose steadystate gains and time constants can be calculated directly from polynomials (2) and (4)

$$G_{11} = \frac{K_1}{T_1 p+1} \quad , \quad G_{12} = \frac{-K_2}{T_2 p+1}$$

$$G_{21} = \frac{K_2 e^{-2NT_\ell p}}{T_2 p+1} \quad , \quad G_{22} = \frac{-K_1}{T_1 p+1} \qquad (5)$$

where $DT = 2NT_\ell$

Under the condition: $\alpha = 1.1$ ($\varepsilon = 0.1$), $N = 10$, $T = 1$ and $T_\ell = 0.2$ the computing results are as follows:

$K_1 = 116.95$, $K_2 = 114.5$

$T_1 = 156.9$, $T_2 = 153$

$DT = 2 \times 10 \times 0.2 = 4.0$

These results are in accord with those approximate model (1). The fact that there is only little difference between either K_1 and K_2 or T_1 and T_2 means the interaction between top and bottom is very strong.

3. Time Domain Analysis:

It is very difficult to inverse transform the transfer function matrix. Therefore the better way to get the time response corresponding to the transfer function is to solve the difference equations by using numerical method.

As shown in the earlier research (1), the difference equations are:

$$\tilde{y}_{n-1} - 2\tilde{y}_n + \tilde{y}_{n+1} - p\tilde{y}_n = \frac{c}{V_r}(\tilde{v} - \alpha \tilde{\ell}_{n-1})$$

$$\tilde{x}'_{n-1} - 2\tilde{x}'_n + \tilde{x}'_{n+1} - p\tilde{x}'_n = \frac{c}{V_r}(\alpha \tilde{v} - \ell'_{n+1}) \qquad (7)$$

where

$$\tilde{\ell}_{n-1} = \tilde{\ell}_o e^{-(n-1)pT_\ell}$$

$$\tilde{\ell}'_{n+1} = \tilde{\ell}_o e^{-(2N-n)pT_\ell}$$

Turning above equations back into time domain yields

$$y_{n-1} - 2\,y_n + y_{n+1} - d\,y_n/dt = \frac{c}{V_r}(v - \alpha \ell_{n-1}) \tag{8}$$

$$x'_{n-1} - 2\,x'_n + x'_{n+1} - d\,x'_n/dt = \frac{c}{V_r}(\alpha v - \ell'_{n+1})$$

Whilst ℓ_{n-1} and ℓ'_{n+1} can be expressed as:

$$\ell_{n-1} = \ell_o\ \nu\{t - (n-1)T_\ell\}$$
$$\ell'_{n+1} = \ell_o\ \nu\{t = (2N-n)T_\ell\} \tag{9}$$

where ν is unit step function.

By using finite difference approximation above equations can be rewritten as explicit formula and for the sake of convenience we set the sampling time interval $h = T_\ell$.

Thus we get

$$y_{n,k+1} = h\{y_{n-1,k} - (2-1/h)y_{n,k} + y_{n+1,k} - \frac{c}{V_r}(v - \alpha\ell_{n-1})\}$$

$$x'_{n,k+1} = h\{x'_{n-1,k} - (2-1/h)x'_{n,k} + x'_{n+1,k} - \frac{c}{V_r}(\alpha v - \ell'_{n+1})\} \tag{10}$$

$$\ell_{n-1} = \ell_o\ \nu\{k - (n-1)\}$$
$$\ell'_{n+1} = \ell_o\ \nu\{k - (2N-n)\} \tag{11}$$

where: $k = \mathrm{INT}(t/h)$.

Similarly the boundary conditions can be expressed as the form of finite difference.

For feed boundary.

$$y'_{N,k+1} = h\{x'_{N,k} - (2-1/h)y_{N,k} + y_{N-1,k} - \frac{c}{V_r}(\frac{\alpha+1}{2}v - \alpha\ell_{N-1})\}$$

$$x'_{N,k+1} = h\{y_{N,k} - (2-1/h)xp_{N,k} + x'_{N-1,k} - \frac{c}{V_r}(\alpha v - \frac{\alpha+1}{2}\ell_N)\} \tag{12}$$

$$\ell_{N-1} = \ell_o\ \nu\{k - (N-1)\} \tag{13}$$
$$\ell_N = \ell_o\ \nu\{k - N\}$$

For the terminal boundary:

$$y_{o,k+1} = \frac{k}{T}\{y_{1,k} + (T/h - \alpha)y_{o,k}\}$$

$$x'_{o,k+1} = \frac{k}{T}\{x'_{1,k} + (T/h - \alpha)x'_{o,k}\} \qquad (14)$$

where T is the residence time of terminals.

Assuming zero initial conditions i.e. $y_{i,o} = o$, $x'_{i,o} = o$ (i=O,1,...N) then setting v = o and $c.\ell_o/V_r = 1$ yields the step response of G_{12} and G_{21}. Similarly, if $\ell_o = o$ and $vC/V_r = 1$ are given, the response of G_{12} and G_{21} can be computed from n = o to n = N.

It is noticeable however that if the hydraulic time constant T_ℓ is greater than O.5 we can no longer set the sampling interval $h = T_\ell$, otherwise the solution will be divergent. In this case we can choose another time interval h which is less than O.5 and the liquid flow ℓ_{n-1} is expressed as

$$\ell_{n-1} = \ell_o\, \nu\{k - (n-1)r\}$$

where $r = T_\ell/h$ is chosen to equal or approximately equal to a integer. The plots of time response (α = 1.1, N = 10, T = 1.0, T_ℓ = O.4) are shown in Fig. 2. These plots show again that the dynamic behaviour of this system is very near to that of first order lag.

It is found from computing results that the steady state gains as $t \to \infty$ are different from those of transfer functions as $p \to o$. For example as α = 1.1, N = 10, T = 1.0 and T_ℓ = O.4 the former are K_1 = 106.46 and K_2 = 104.04 while the latter are K_1 = 117.09 and K_2 = 114.39 (the error is about 10 percent). These errors are caused from the improper differential approximation of the difference equation of feed boundary conditions. In fact it has been tested by computing that if we take $y_N - y_{N-1} \doteq \left.\frac{dy}{dn}\right|_{n=N-1}$ instead of $y_N - y_{N-1} \doteq \left.\frac{dy}{dn}\right|_{n=N}$, the errors will vanish. The results of solving difference equations (7) as below are in accord with that of numerical method.

4. Solution of Difference Equation

The usual method used to describe a tray-type column is difference equations. Therefore solving them directly should be the better way to get the T.F.M.

The difference equations (7) is rewritten as follows:

$$\tilde{y}_{n-1} - (p+2)\tilde{y}_n + \tilde{y}_{n+1} = \frac{c}{V_r}\{\tilde{v} - \alpha\,\tilde{\ell}_o e^{-(n-1)pT_\ell}\}$$

$$\tilde{x}_{n-1} - (p+2)\tilde{x}'_n + \tilde{x}'_{n+1} = \frac{c}{V_r}\{\alpha\,\tilde{v} - \tilde{\ell}_o\, e^{-(2N-n)pT_\ell}\}$$

The terminal boundary condition is:

$$\tilde{y}_1 = (pT + \alpha)\tilde{y}_o$$

$$\tilde{x}' = (pT + \alpha)\tilde{x}'_o$$

The feed boundary condition is:

$$\tilde{x}'_N - (p+2)\tilde{y}_N + \tilde{y}_{N-1} = \frac{c}{V_r}\{\frac{\alpha+1}{2}\,\tilde{v} - \alpha\,\tilde{\ell}_o\, e^{-(N-1)pT_\ell}\}$$

$$\tilde{y}_N - (p+2)\tilde{x}'_N + \tilde{x}'_{N-1} = \frac{c}{V_r}\{\alpha\,\tilde{v} - \frac{\alpha+1}{2}\,\tilde{\ell}_o\, e^{-NpT_\ell}\}$$

This is a set of second order difference equations and can be solved by ordinary technique (3). The solutions are listed as follows:

$$Q = G_d F$$

where

$$Q = \begin{pmatrix} \tilde{y}_o \\ \tilde{x}'_o \end{pmatrix} \qquad F = \begin{pmatrix} \ell_o \\ v \end{pmatrix} \qquad = \frac{c}{V_r} \qquad \text{as before}$$

G_d is the transfer function matrix from difference equation.

$$G_d = A^{-1}B \tag{15}$$

And the matrix A and B have the forms as follows:

$$A = \begin{pmatrix} (p+2)F_1 - F_5 & -F_1 \\ -F_1 & (p+2)F_1 - F_5 \end{pmatrix}$$

$$B = \begin{pmatrix} \alpha e^{-(N-1)pT_\ell} - (p+2)F_3 + F_7 + F_4 & \alpha F_2 + F_6 - \frac{\alpha+1}{2} - (p+2)F_2 \\ \frac{\alpha+1}{2} e^{-NpT_\ell} - (p+2)F_4 + F_8 + F_3 & F_2 + \alpha F_6 - \alpha - \alpha(p+2)F_2 \end{pmatrix}$$

The complex functions $F_1 - F_8$ can be expressed as:

$$F_1 = (pT + \alpha)\ \phi(N) - \phi(N-1)$$

$$F_2 = \{\phi(N) - \phi(N-1) - 1\}/P$$

$$F_3 = \{e^{-pT_\ell}\ \phi(N) - \phi(N-1) - e^{-NpT_\ell}\}\alpha/D_1$$

$$F_4 = \{e^{pT_\ell}\phi(N) - \phi(N-1) - e^{NpT_\ell}\}.\ e^{-(2N-1)pT_\ell}/D_2$$

$$F_5 = (pT + \alpha)\ \phi(N-1) - \phi(N-2)$$

$$F_6 = \{\phi(N-1) - \phi(N-2) - 1\}\ /p$$

$$F_7 = \{e^{-pT_\ell}\phi(N-1) - \phi(N-2) - e^{-NpT_\ell}\}\alpha/D_1$$

$$F_8 = \{e^{pT_\ell}\phi(N-1) - \phi(N-2) - e^{NpT_\ell}\}e^{-(2N-1)pT_\ell}/D_2$$

$$D_1 = e^{-2pT_\ell} - (p+2)e^{-pT_\ell} + 1$$

$$D_2 = e^{2pT_\ell} - (p+2)e^{pT_\ell} + 1$$

The complex function ϕ is defined as;

$$\phi(n) = \frac{r_1^n - r_2^n}{r_1 - r_2} \qquad (16)$$

where:

$$r_1, r_2 = \frac{(p+2) \pm \sqrt{(p+2)^2 - 4}}{2}$$

They are the characteristic roots of above difference equations (2).

The hyperbolic function in the earlier research (1) is substituted by the function $\phi(n)$ here. These solutions are more exact than that of the earlier one (1). Especially as $T_\ell = 0$ the T.F.M. can be reformed as a diagonal form. The elements of its main diagonal line are

$$G_{11}(p) = \frac{\{(p+3)\phi(N)-(p+4)\phi(N-1)+\phi(N-2) - 2\} - 0.5\varepsilon}{(p+3)(pT+\alpha)\phi(N)-(pT+p+\alpha+3)\phi(N-1)+\phi(N-2)} \qquad (17)$$

$$G_{22}(p) = \frac{-\{(p+1)\phi(N)-(p+2)\phi(N-1)+\phi(N-2)\}(\alpha+1)/p - 0.5\varepsilon}{(p+1)(pT+\alpha)\phi(N)- pT+p+\alpha+1)\phi(N-1)+\phi(N-2)}$$

Their zero frequency behaviour are

$$G_{11}(o) = \frac{N^2\varepsilon - 0.5\varepsilon}{2\varepsilon N +\alpha+ 1}$$

$$G_{22}(o) = - \frac{N(\alpha+1)+0.5\varepsilon}{\varepsilon} \qquad (18)$$

The numerators of above expression (18) are less than those of the results in earlier research (2). In fact the computing results of T.F.M (G_d) under the conditions α= 1.1 (ε = 0.1), N = 10, T = 1.0 and T_ℓ = 0.2 show an obvious difference between the solutions of this difference equation and those of the differential equation (1). The error at zero frequency is about 10% and increases with frequency.

The values of the T.F.M. (12) at zero frequency are exactly equal to those results of numerical method as $t \to \infty$. This is in accord with the final value theorem.

5. Conclusion and discussion

The analysis of the T.F.M. in the frequency domain predicts that the distillation column system (compositions to terminal flow rate) is a low pass filter with large time constants and low cut-off frequency (about 0.08). So studying its low frequency behaviour has the more practical significance.

The computed results in both frequency and time domains further reveal the strong resemblance of the dynamic behaviour of this system to that of first order lag both qualitatively and quantilatively. Furthermore, at low frequency the elements of the T.F.M. can be expanded by Taylor theorem, into approximate analytical model of a first-order-lag type whose steady-state gains and time constants can be calculated directly from

those polynomials of the parameters α, N and T. The dead time of the elements G_{21} equals to the product of hydraulic time constant T_ℓ and total stage number i.e. DT = 2NT while the time lags of the other elements are negligible.

The fact that solving difference equations directly can get more exact results shows that the better way to describe a tray-type distillation column in frequency domain is to use difference equation. There is no need to use differential equations to approximate the difference equation.

6. References

(1) Zhou, B.M., Wang, A.M. and Edwards, J.B., 'The influence of hydraulic delay on the composition dynamics and controller design of tray-type distillation columns', Research Report No. 209, January, 1983.

(2) Edwards, J.B. and Tabrizi, M.H.N.'An analytically-derived, parametric transfer-function model for ideal, tray-type, binary distillation columns', Trans. I. Chem. E.

(3) Derosso, Paul M. 'State variables for Engineers' 1965, (New York, London, Sydney) pp. 83-100

(4) Rademaker, O., Rijnsdorp, J.E. and Manrleveld, A. 'Dynamics and control of continuous distillation units', Amsterdam - Oxford - New York 1975.

Fig. 1-1 INVERSE NYQUIST LOCUS OF G_{11}

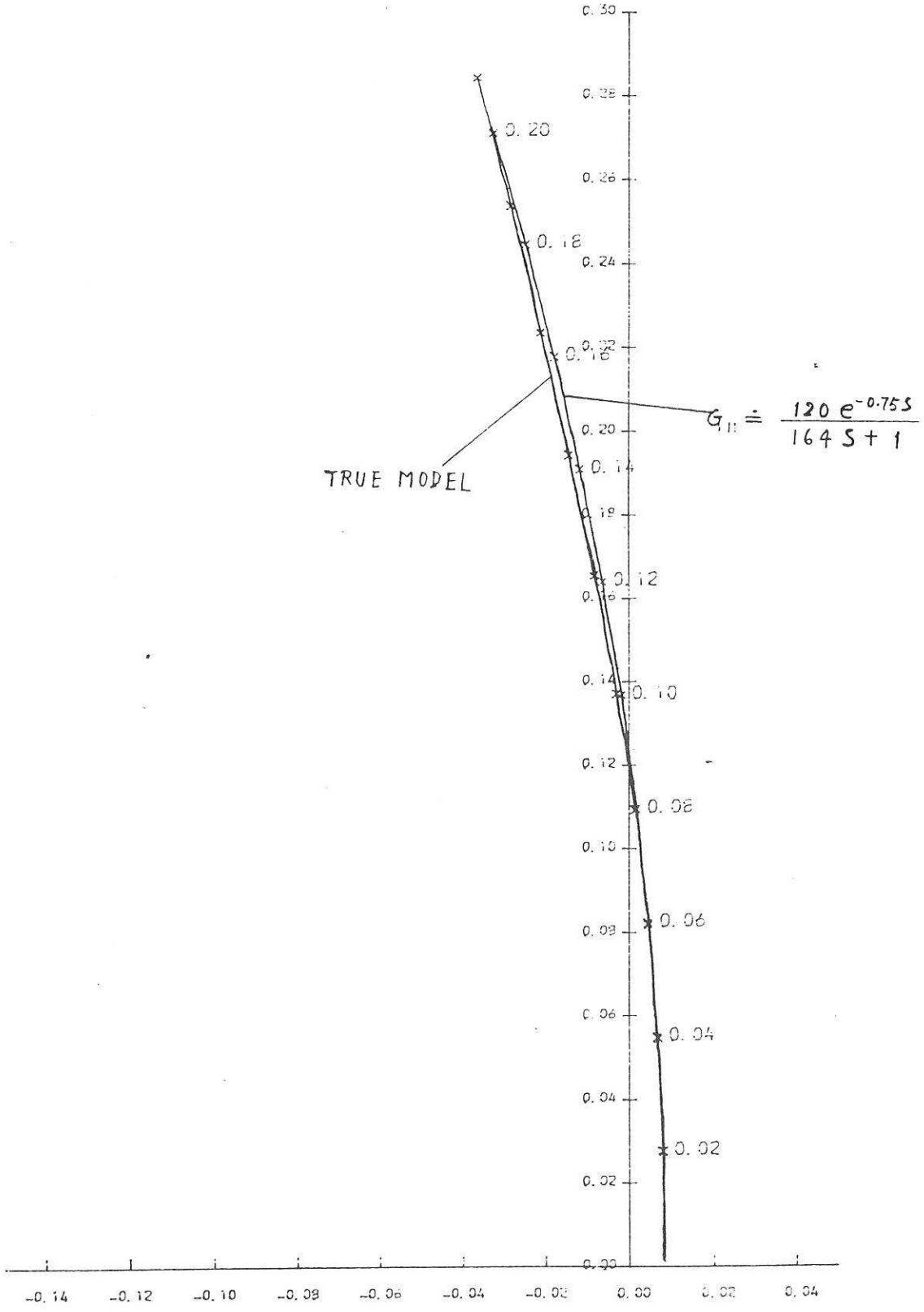

Fig. 1-2 INVERSE NYQUIST LOCUS OF G12

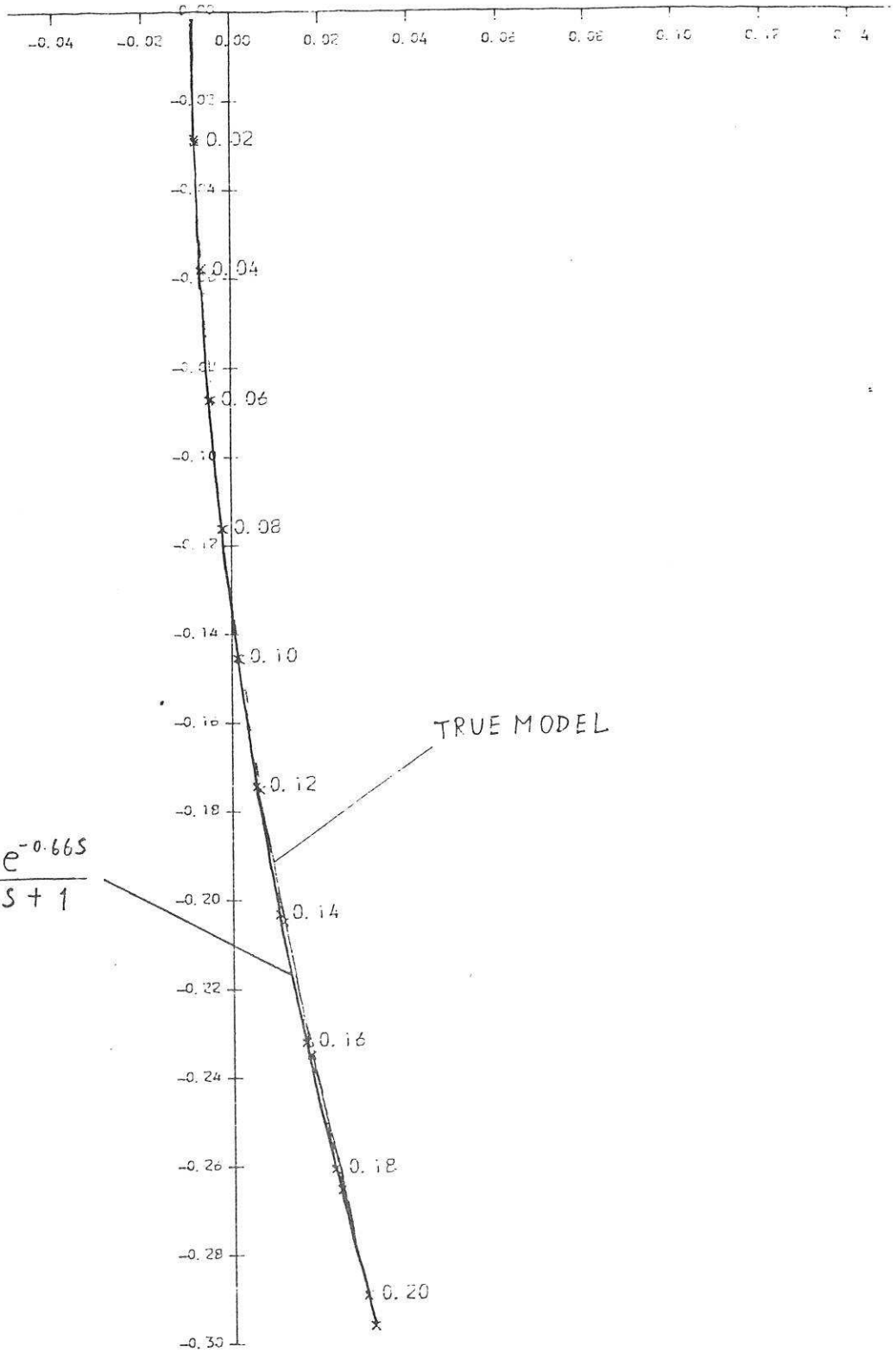

Fig. 1-3 INVERSE NYQUIST LOCUS OF G_{21}

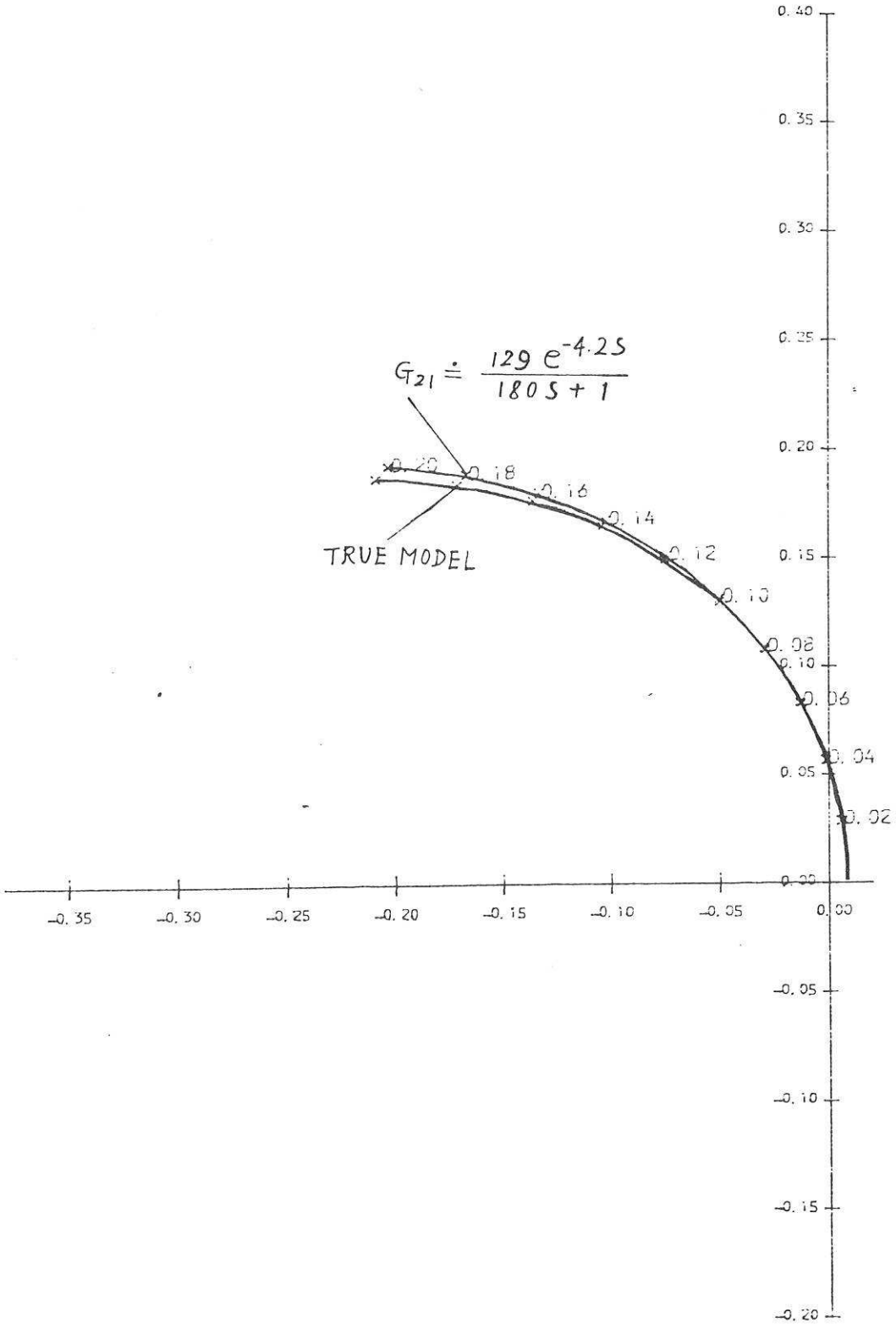

Fig. 1 - 4 INVERSE NYQUIST LOCUS OF G22

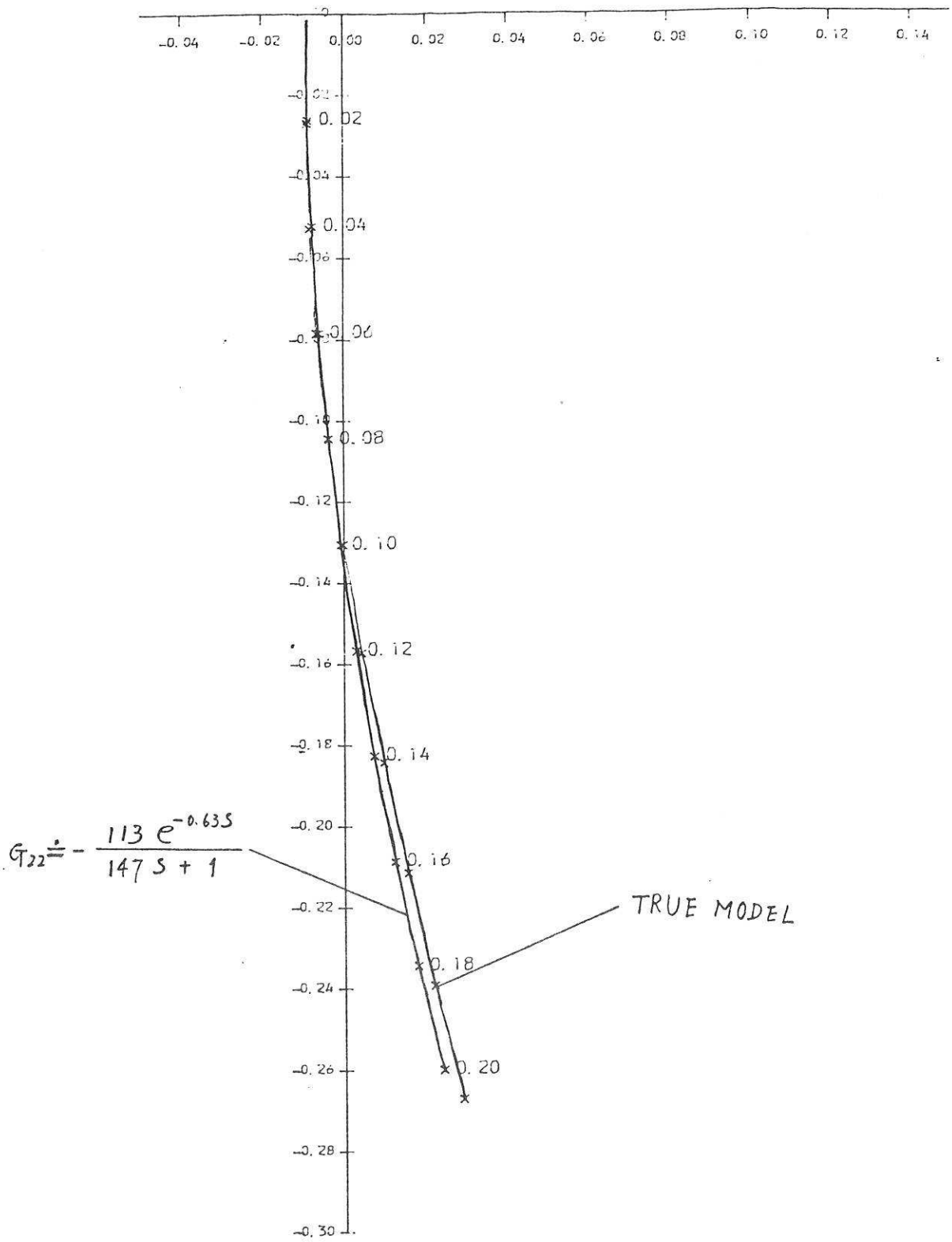

Fig. 2 - 1 THE STEP RESPONSE CURVE OF G11

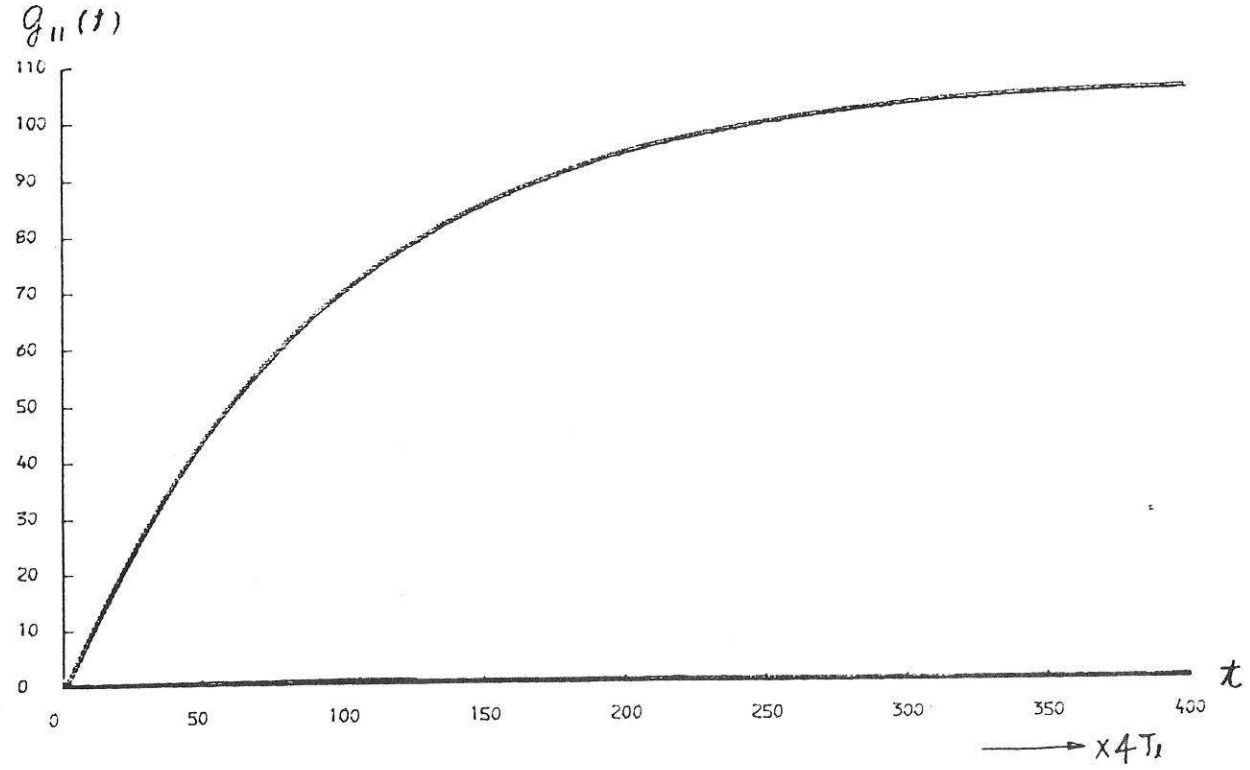

Fig. 2 - 3 THE STEP RESPONSE CURVE OF G21

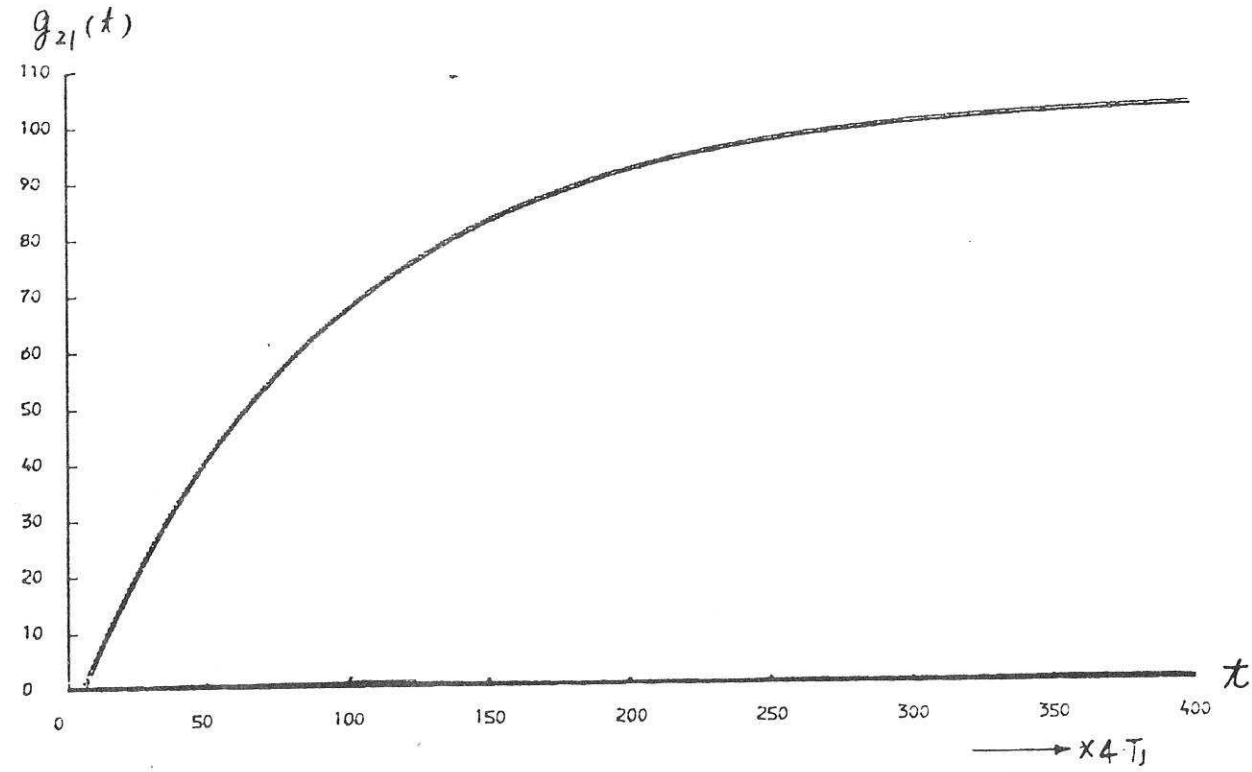

Fig. 2-2 THE STEP RESPONSE CURVE OF G12

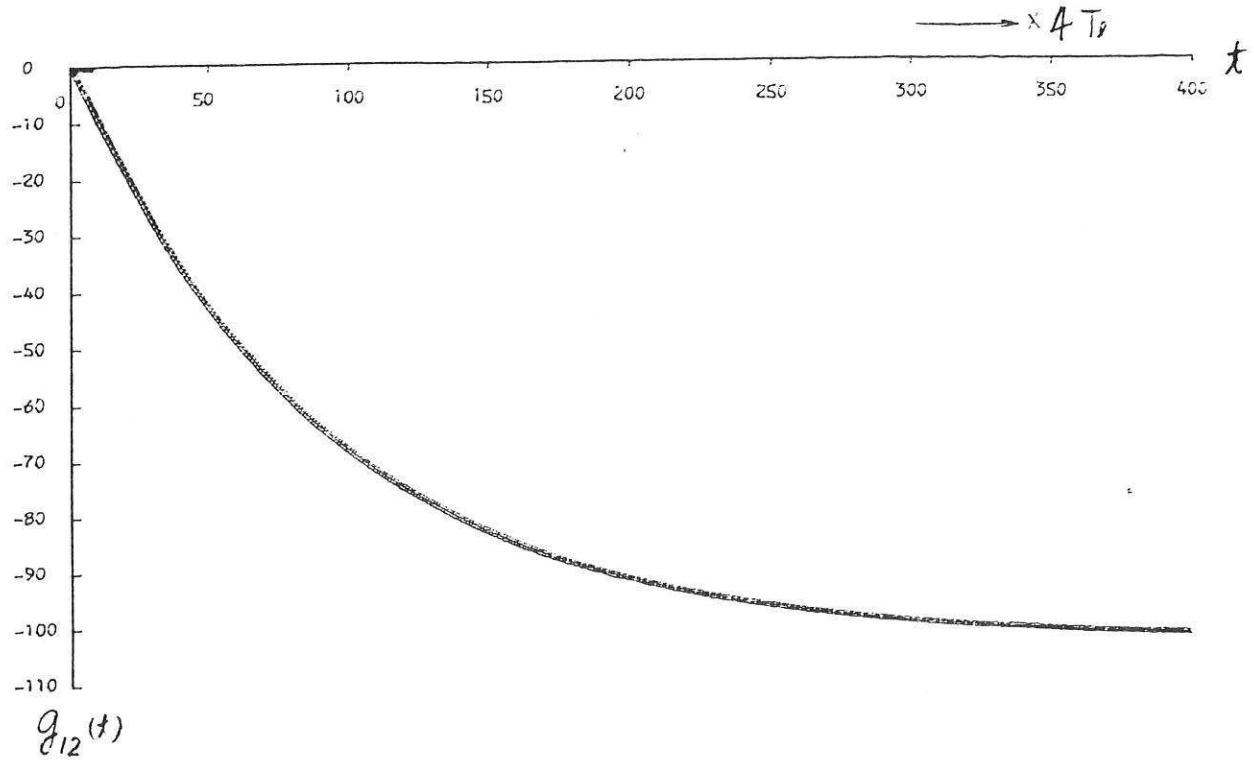

Fig. 2-4 THE STEP RESPONSE CURVE OF G22

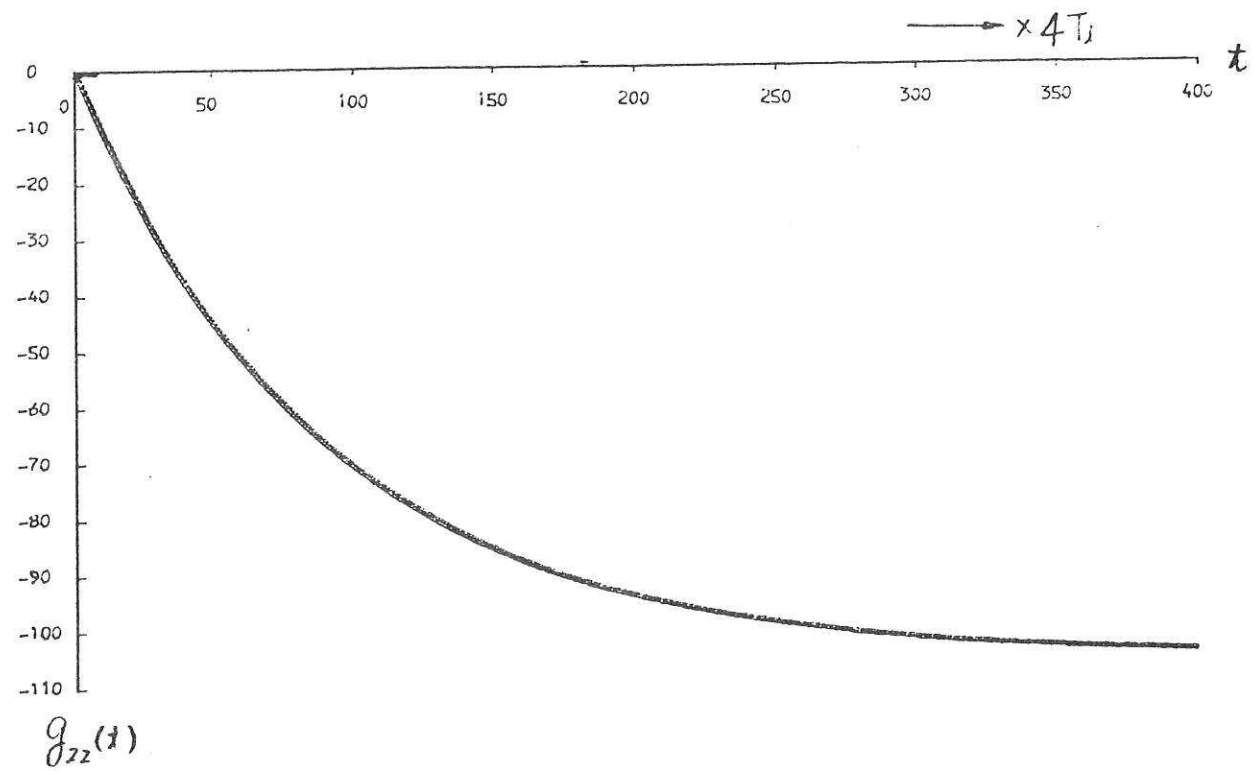

Fig. 3 - 1 INVERSE NYQUIST LOCUS OF G^*_{11}

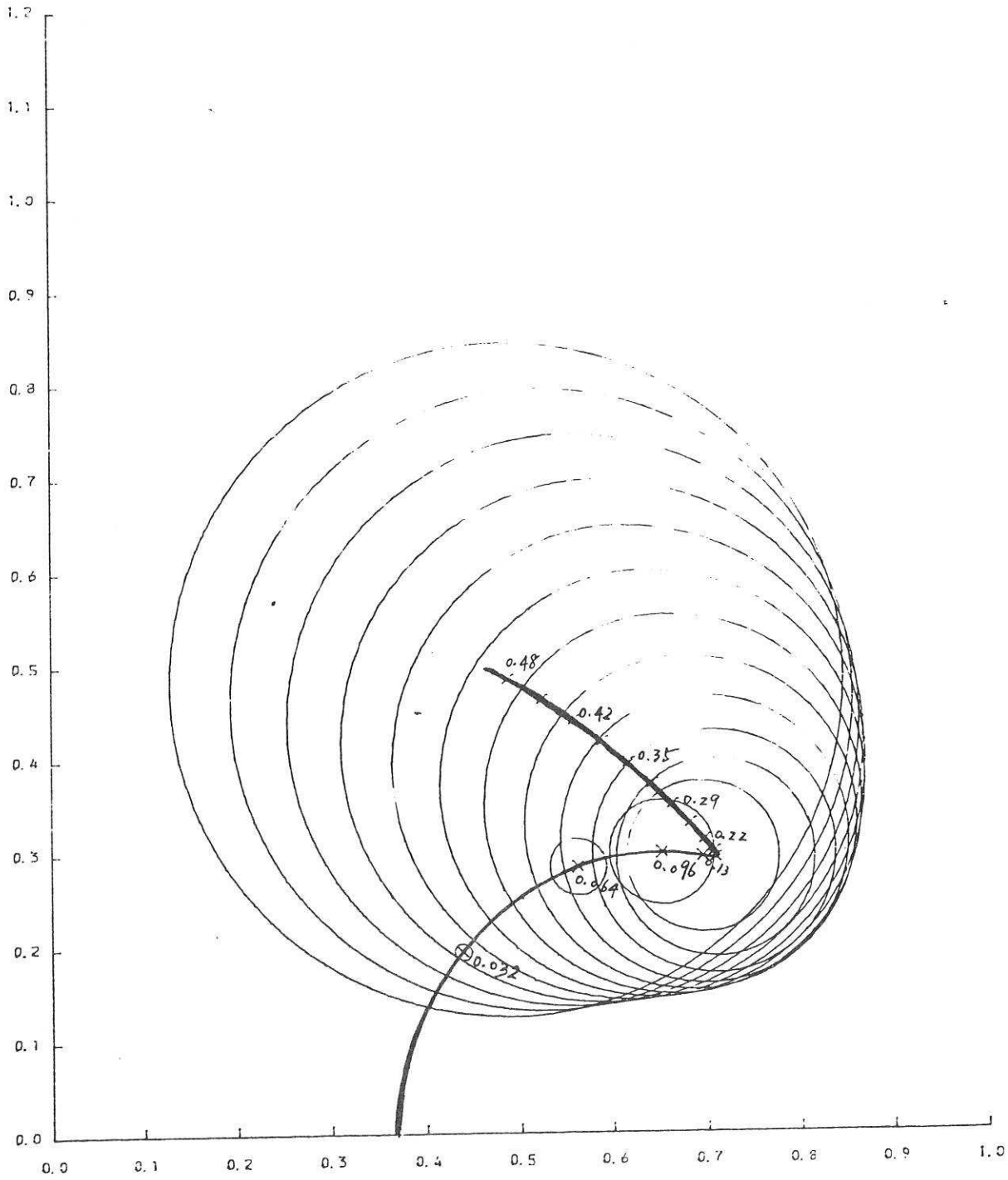

Fig. 3-2 INVERSE NYQUIST LOCUS OF G^*_{22}

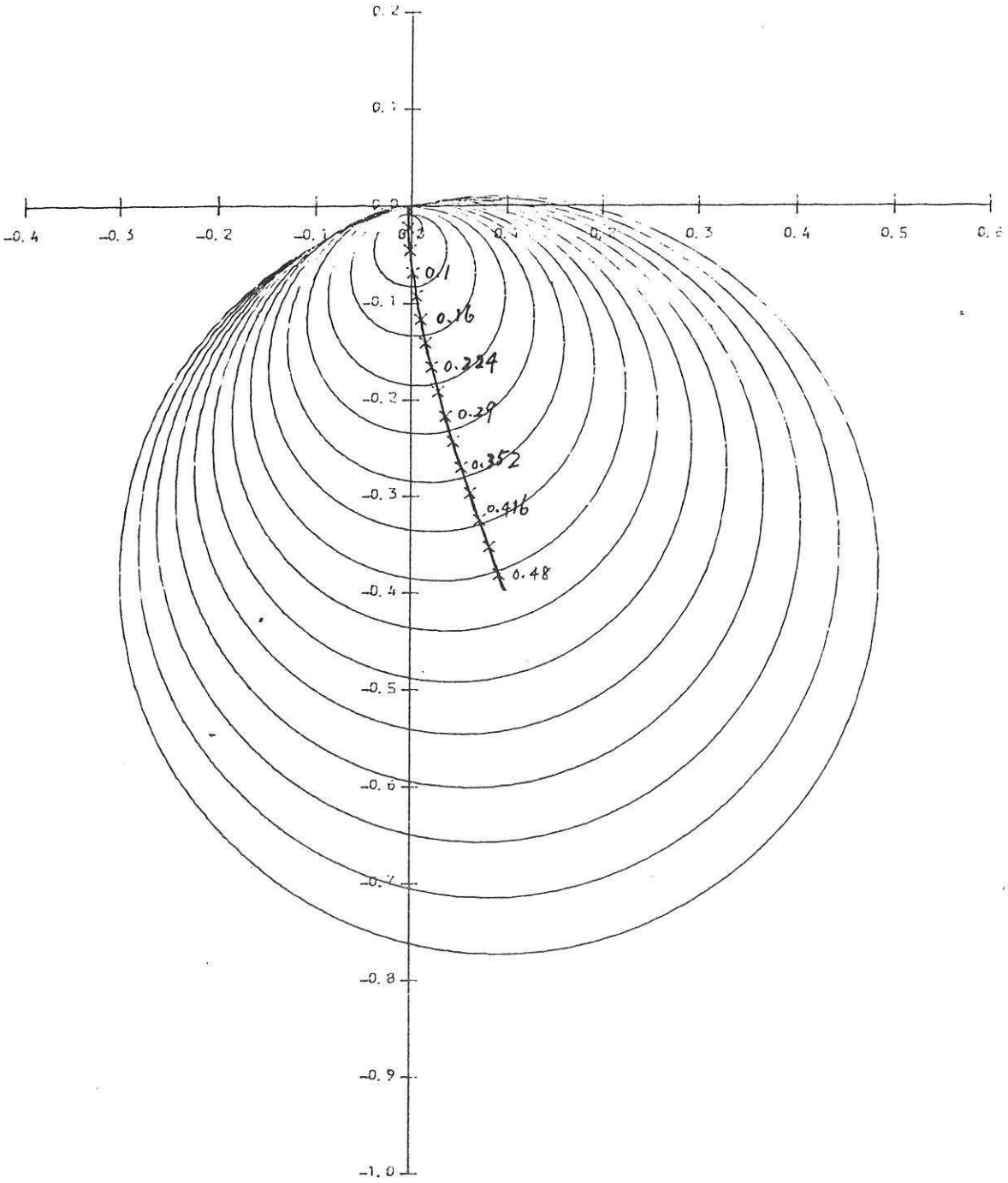

Fig. 4 INVERSE NYQUIST LOCUS OF G21